Structural and mechanistic analyses of yeast mitochondrial thioredoxin Trx3 reveal putative function of its additional cysteine residues

Rui Bao [a], Yaru Zhang [a], Cong-Zhao Zhou [b,c], Yuxing Chen [a,b,c,*]

[a] Institute of Protein Research, Tongji University, Shanghai, 200092, PR China
[b] Hefei National Laboratory for Physical Sciences at Microscale, PR China
[c] School of Life Sciences, University of Science and Technology of China, Hefei, Anhui, 230027, PR China

ARTICLE INFO

ABSTRACT

The yeast Saccharomyces cerevisiae Trx3 is a key member of the thioredoxin system to control the cellular redox homeostasis in mitochondria. We solved the crystal structures of yeast Trx3 in oxidized and reduced forms at 1.80 and 2.10 Å, respectively. Besides the active site, the additional cysteine residue Cys69 also undergoes a significant redox-correlated conformational change. Comparative structural analyses in combination with activity assays revealed that residue Cys69 could be S-nitrosylated in vitro. S-nitrosylation of Cys69 will decrease the activity of Trx3 by 20%, which is comparable to the effect of the Cys69Ser mutation. Taken together, these findings provided us some new insights into the putative function of the additional cysteine residues of Trx3.

© 2009 Elsevier B.V. All rights reserved.

1. Introduction

Thioredoxin (Trx), thioredoxin reductase and NADPH consist of the most important system to control the cellular redox homeostasis in all organisms. Thioredoxins have been found to perform various physiological functions such as disulfide oxidoreductase for ribonucleotide reductase [1], gene expression regulator [2], control factor participating in filamentous phage assembly [3], biosynthesis of cysteine and methionine [4], antioxidant during oxidative stress [5] and cytotoxicity enhancing factor in a truncated form [6]. These physiological and biochemical activities of Trx are based on its broad substrate specificity and powerful reducing capacity [7]. In addition, human cytoplasmic Trx1 has been proven to play a central role in cellular S-nitrosylation events via its additional cysteine residues Cys69 and/or Cys73 rather than those two at the active site [8–10]. Moreover, recent reports have proven that yeast mitochondria are capable of producing NO under hypoxic conditions and presented an environment for protein S-nitrosylation [11–17].

Trx3/YCR083W is the third isoform of yeast thioredoxin, residing in mitochondria. Studies of Saccharomyces cerevisiae mutant strains revealed that the TRR2 null mutant was more sensitive to H_2O_2, and TRX3 null mutant was as sensitive as the wild type, indicating that mitochondrial thioredoxin system was important in protection against oxidative stress [18]. Notably, Trx3 possesses two additional cysteine residues Cys57 and Cys69, compared with Trx1 and Trx2. To decipher the putative function of these additional cysteine residues, we solved the crystal structures of yeast Trx3 in reduced and oxidized forms. Comparison between the two structures revealed remarkable variations around the additional cysteine residues besides the active site. Furthermore, in vitro activity assays proved that either mutation or S-nitrosylation of Cys69 would decrease the activity of Trx3. These findings gave us some hints about the putative role of yeast Trx3 via S-nitrosylation of its additional cysteine residue Cys69.

2. Materials and methods

2.1. Cloning, expression and purification

Mature form of yeast Trx3 and Trr2 with hexahistidine (6×His) tags were overexpressed in Escherichia coli BL21 (DE3) and purified as described previously [18,19]. The Trx3C57S, Trx3C69S and Trx3C57S/C69S mutageneses were carried out by PCR as described [20] and the proteins were purified using the same protocol. The reduced form of Trx3 (Trx3-red) was obtained by incubating the protein in the storage buffer (100 mM NaCl, 50 mM Tris–HCl, pH 8.0) plus 8 mM DTT for 30 min at 4 °C. The oxidized form (Trx3-ox) was produced by incubating Trx3 in the storage buffer containing 10 mM oxidizing agent diamide (azodicarboxylic acid bis(dimethylamide), SIGMA) for 30 min at room temperature. After oxidation, diamide

* Corresponding author. Institute of Protein Research, Tongji University, Shanghai, 200092, PR China.
E-mail address: cyxing@ustc.edu.cn (Y. Chen).

was removed by gel filtration using a Hi-load 16/60 Superdex 75 column (Amersham Biosciences) equilibrated against the storage buffer. Eluted protein fractions were concentrated to 15 mg/ml. The wild type and mutants of Trx3 for activity assay were purified without reducing regents, concentrated to 20 mg/ml and kept in storage buffer.

2.2. Crystallization

Two forms of Trx3 protein were crystallized at 18 °C using hanging-drop vapor diffusion method. In each hanging drop, 2 μl of protein was mixed with 2 μl precipitant solution, screened with Crystal Screen I and II (Hampton Research Inc.). Crystals of Trx3-red were found from the condition of 0.2 M ammonium sulfate, 0.1 M sodium acetate, pH 4.6, 8% (w/v) PEG 4000 and 15% glycerol [19], and optimized in the same condition. Crystals of Trx3-ox were grown in 0.2 M $MgCl_2$, 0.1 M HEPES, pH 7.0, 30% PEG 4000 for 1 week, and a single crystal ($0.1 \times 0.1 \times 0.05$ mm^3) suitable for data collection were obtained within 3 days after seeding crashed crystals into drops pre-equilibrated against the buffer of 30% PEG 4000, 0.2 M Li_2SO_4, 0.1 M Tris–HCl, pH 8.5.

2.3. X-ray data collection, structure solving and refinement

The crystals were transferred to the reservoir solution plus 15%–20% glycerol and flash frozen under a nitrogen stream. Diffraction data were collected at 100 K on an R-AXIS IV^{++} image-plate detector using Rigaku rotation-anode generator (Cu Kα radiation operated at 50 kV and 100 mA, Rigaku Japan). Data were indexed and integrated with MOSFLM [21] and scaled by SCALA of CCP4 suite 6.0 [22].

The homology model was generated from human Trx1 (PDB code: 1ERV). The structures were solved by rotation/translation searches with CNS 1.1 [23], Further refinement was carried out using Refmac5 of CCP4 [22]. Alternatively, manual rebuilding and water relocation were performed with O [24]. The stereochemistry of the models was calculated with PROCHECK [22]. Final coordinates and structure factors have been deposited in the Protein Data Bank under the accession code of 2OE1 and 2OE3 (http://www.rcsb.org/pdb). The data collection statistics and processing results were summarized in Table 1.

2.4. Determination of S-nitrosylation and activity assay

The fresh S-nitrosoglutathione (GSNO) was prepared as described [25]. The purified Trx3, Trx3C57S and Trx3C69S at a concentration of about 100 μM were pretreated with 1 mM diamide to form a disulfide bond between the active site residues Cys32 and Cys35, and then mixed with 15 mM GSNO, respectively. After incubating for 2 h at 30 °C, the excess GSNO was removed by desalting. GSNO-treated samples were determined by spectrophotometry at 335 nm, and the S-nitrosothiol (SNO) contents were determined using the Griess–Saville method [26,27]. The concentration of protein samples were determined by absorbance at 280 nm (extinction coefficient value: 10,400 M^{-1} cm^{-1}).

The kinetic values of Trx3 and its mutants with the substrate bovine insulin were calculated as described [28] with some modifications: the reactions containing 100 mM PBS, pH 7.0, 2 mM EDTA, 0.1 μM Trr2, 0.25 mM NADPH, 0.5 μM of Trx3 or mutants were triggered by the addition of various concentrations of insulin (0.7–140 μM) and the A_{340} decrease was monitored for 5 min at 28 °C, using an extinction coefficient value of 6220 M^{-1} cm^{-1} for NADPH. Each assay was repeated twice.

3. Results and discussion

3.1. Data statistics and overall structure

Crystal structures of yeast Trx3 were solved by molecular replacement. These structures represent Trx3 at oxidized and reduced forms, thus termed Trx3-ox and Trx3-red accordingly. Both of them have two molecules in an asymmetric unit. The overall electron density maps are fitted well in both structures, including residues from Tyr1 to Leu104. The data collection and refinement statistics are listed in Table 1.

Similar to all thioredoxins of known structure, Trx3 displays a typical Trx fold with three parallel and two antiparallel β-strands surrounded by four α-helices (Fig. 1A) [29–35]. The primary sequence of Trx3 is ~46% identical to that of human Trx1, and ~31% to E. coli TrxA. Superposition of Cα atoms of Trx3-red with the reduced human Trx1 and E. coli TrxA gave an RMSD of 1.12 Å and 1.26 Å, respectively. In addition, the C-terminal of helix α2 is variable as observed in previous structures, which was presumed to significantly influence ionization of the cysteine thiol and stabilization of the thiolate [36].

3.2. Comparison of the oxidized and reduced molecules of Trx3

The distances between Cys32 and Cys35 Sγ atoms in Trx3-ox are 2.07 and 2.10 Å in the two molecules of an asymmetric unit, respectively, representing the typical length of disulfide bond, whereas those in Trx3-red are 3.67 and 3.71 Å, respectively. Molecule A of Trx3-red and molecule B of Trx3-ox display the largest variation, thus were used as the reduced and oxidized model through structure analyses, respectively. Although the overall RMSD of Cα atoms between Trx3-ox and Trx3-red is only 0.63 Å, this difference is significant compared to other pairs of reduced/oxidized Trx structures from various species, which are in the range from 0.15

Table 1
Data collection and crystallographic statistics

	Oxidized Trx3 (Trx3-ox)	Reduced Trx3 (Trx3-red)
Data processing		
Space group	$P2_12_12_1$	$P3_1$
Unit cell parameters		
a, b, c (Å)	49.31, 60.68, 72.68	49.58, 49.58, 94.55
α, β, γ (°)	90, 90, 90	90, 90, 120
Resolution (Å)	29.25–1.8 (1.86–1.80)^a	25.41–2.1 (2.21–2.10)
Unique reflections	20,520 (1,880)	14,192 (2,040)
Completeness (%)	98.2 (96.9)	93.5 (91.9)
$I/\sigma(I)$	14.8 (3.6)	14.4 (3.6)
R_{merge} (%)^b	6.2 (34.8)	11.1 (39.3)
Refinement statistics		
Resolution (Å)	29.25–1.80 (1.85–1.80)	25.41–2.10 (2.15–2.10)
R_{work}^{c}	0.19 (0.27)	0.16 (0.18)
R_{free}^{d}	0.25 (0.33)	0.22 (0.32)
Contents of asymmetric unit		
Protein atoms	1645	1657
Water atoms	180	180
RMSD geometry^e		
Bond lengths (Å)	0.014	0.017
Bond angles (°)	1.399	1.565
Average of B factors (Å^2)	21.19	16.65
Ramachandran plot^f		
Most favored (%)	98.54	98.56
Additional allowed (%)	1.46	1.44
Outliers (%)	0	0
PDB entry	2OE3	2OE1

^{a} The values in parentheses refer to statistics in the highest bin.
^{b} Rmerge=∑hkl∑i|Ii(hkl)−<I(hkl)>|/∑hkl∑iIi(hkl), where Ii(hkl) is the intensity of an observation and <I(hkl)> is the mean value for its unique reflection. Summations are over all reflections.
^{c} R-factor=∑h|Fo(h)−Fc(h)|/∑hFo(h), where Fo and Fc are the observed and calculated structure-factor amplitudes, respectively.
^{d} R-free was calculated with 5% of the data excluded from the refinement.
^{e} Root-mean square-deviation from ideal values.
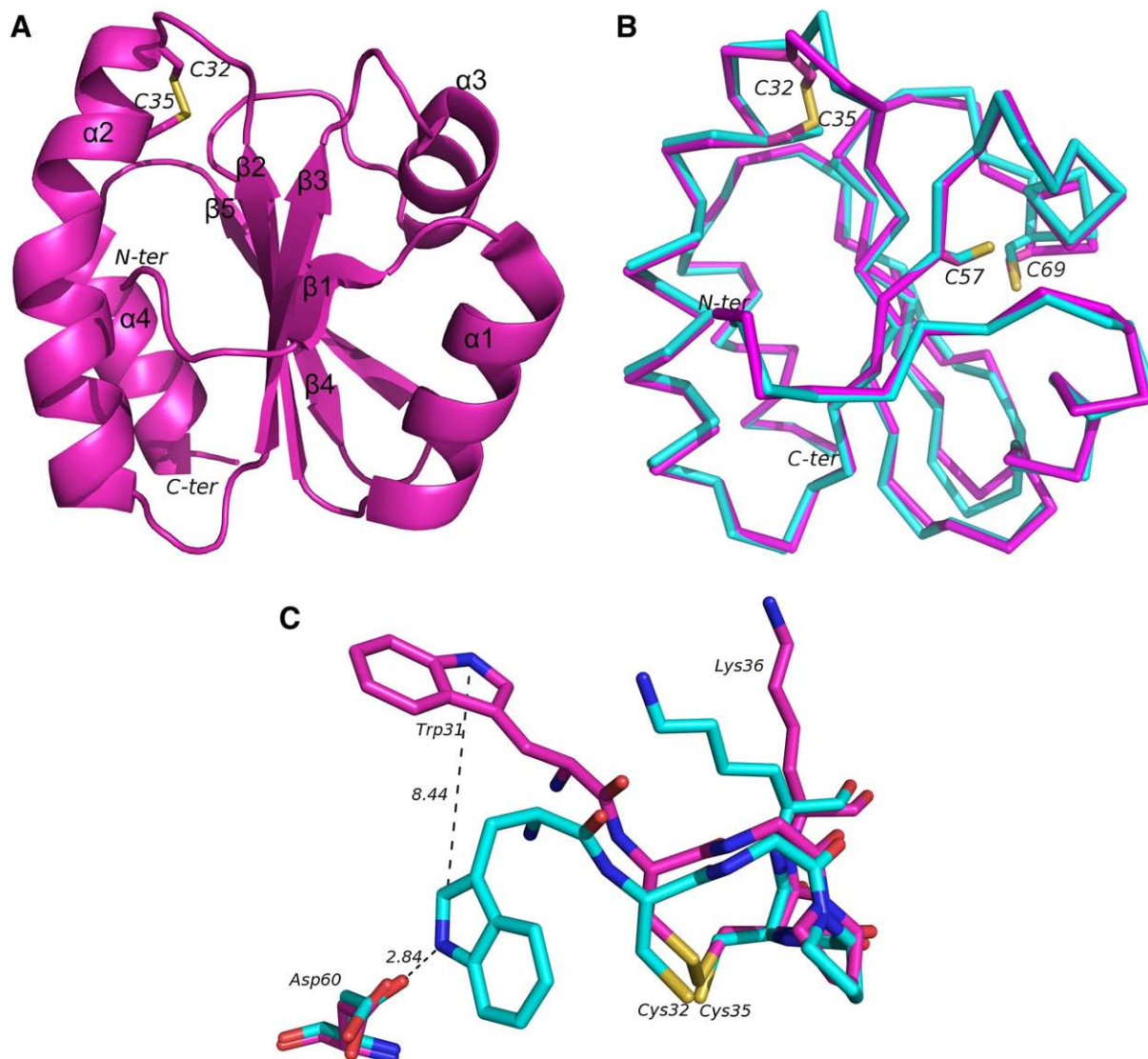^{f} Categories were defined by Molprobity.

Fig. 1. A) Overall structure of Trx3-ox. B) Superposition of the main chain between Trx3-red subunit A (cyan) and Trx3-ox subunit B (magenta). Cysteine residues are labeled and shown in sticks. C) Superposition of the active sites of Trx3-red (molecule B) (in cyan) and Trx3-ox (molecule B) (in magenta), shown in stick. The molecules are colored by atom type. The hydrogen bond between Asp60-Oδ2 and Trp31-Nϵ1 in reduced state is shown in black dash. The figures were made using PyMOL [44].

to 0.29 Å [30–33]. This relatively significant conformational change might be due to the sufficient oxidation/reduction of protein samples prior to crystallization.

Superposition of Trx3-ox molecule B against Trx3-red molecule A revealed two regions (residues Lys67-Ala73, RMSD 0.94 Å; residues Asp82-Gln84, RMSD 1.94 Å) of relatively higher RMSD value, in addition to the active site (residues Thr30-Cys35, RMSD 0.67 Å) (Fig. 1B). In Trx3-red, the conserved Trp31 of WCGPC motif presents a consistent position restrained by its hydrogen bond with Asp60 (Fig. 1C). Upon oxidation, Trp31 adopts an extending conformation and its Nϵ atom shifts about 8.44 Å from that in Trx3-red. The indole ring of Trp31, after rotating 170°, inserts into a hydrophobic pocket of the neighboring subunit generated by a symmetric operation, leading to a large conformational change at the region of Asp82-Gln84.

3.3. Activity assays of Cys57Ser and Cys69Ser mutants

Previous studies on human Trx1 have shown that the additional cysteine residues have considerable effects on the activity resulted from the second disulfide between Cys62 and Cys69 [37], disulfide bonded dimerization via Cys73 [30,38], or S-nitrosylation of Cys69 and/or Cys73 [8,9]. Compared to its paralogs Trx1 and Trx2, yeast Trx3 contains two extra Cys residues (Cys57 and Cys69) besides the highly conserved two at the active site. The residues around Cys69 also undergo significant conformational changes between Trx3-red and Trx3-ox (Fig. 1B), indicating their potential role in redox reactions.

To verify the effects of Cys57 and Cys69 on Trx3 reduction activity, three mutants Trx3C57S, Trx3C69S and Trx3C57S/C69S were constructed. Unfortunately, the double mutant Trx3C57S/C69S was

Table 2
Kinetic parameters of Trx3, Trx3–SNO, Trx3C69S and Trx3C57S towards insulin

	K_m (μM)	k_{cat} (min^{-1})	k_{cat}/K_m (μM^{-1} min^{-1})	Turnover at 140 μM insulin (μM min^{-1})
Trx3	7.15±0.85	17.84±0.56	2.50	8.42±0.11
Trx3C69S	5.69±0.46	12.44±0.23	2.19	6.06±0.07
Trx3C57S	6.56±0.75	13.65±0.36	2.10	6.25±0.08
Trx3–SNO	4.80±0.54	11.67±0.28	2.43	5.43±0.06

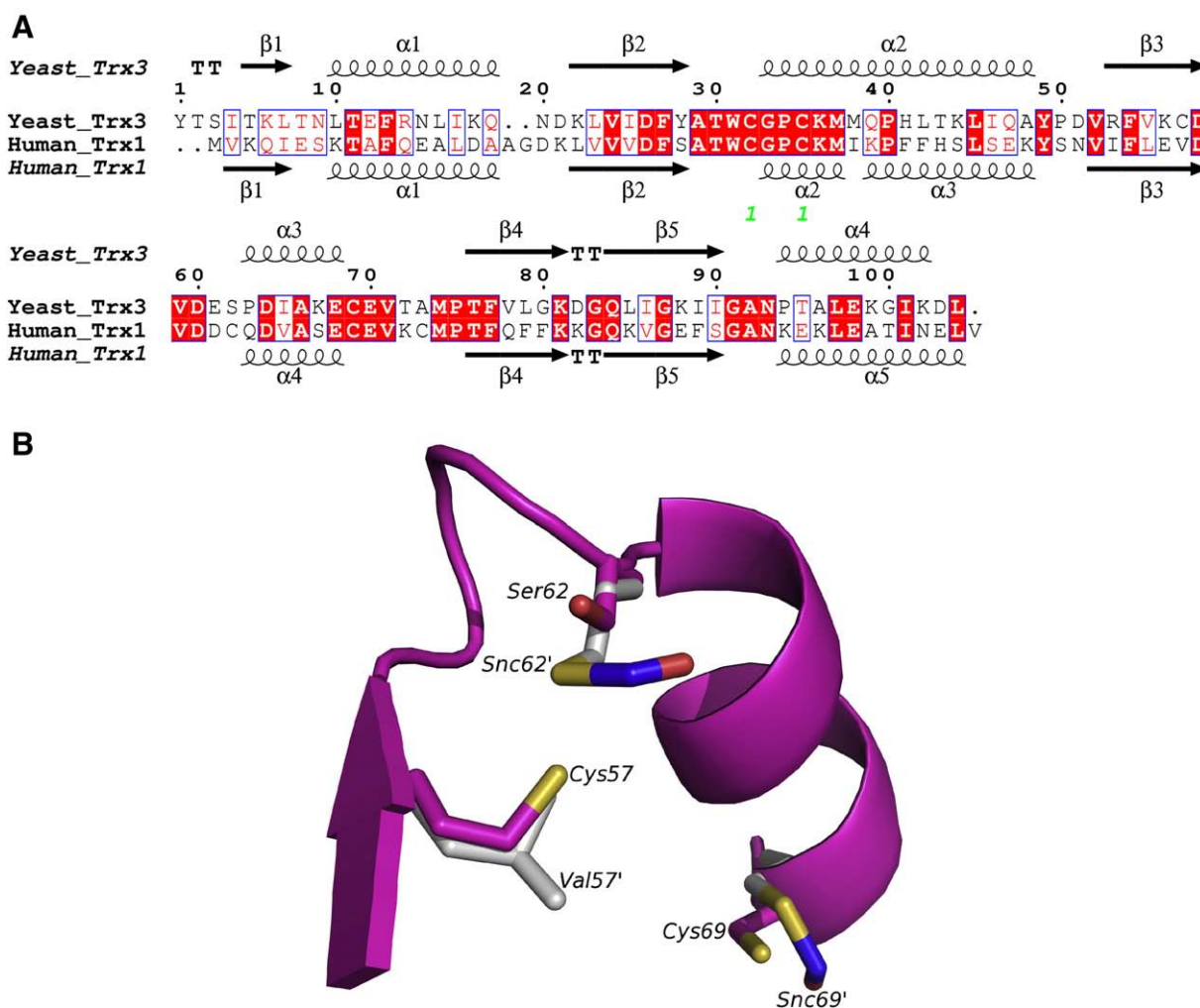The mean value derived from Hill function with a Hill coefficient of 1.

Fig. 2. A) Superposition of the regions around the additional cysteines of Trx3-ox and S-nitrosylated human Trx1. S-nitrosylated human Trx1 (PDB code: 2IIY) is colored in light gray and Trx3-ox in magentas. Residues in human Trx1 are numbered with prime and S-nitrosylated cysteines of human Trx1 are labeled as Snc62′ and Snc69′. The figures were made using PyMOL. B) Sequence alignment of yeast Trx3 (PDB code: 2EO3) and human Trx1 (PDB code: 1ERU) with their secondary structures indicated. The figure was prepared with ESPript [45] and the alignment was performed using CLUSTAL X [46].

overexpressed in *E. coli* as inclusion body, thus only the single mutants could be applied to activity assays. The different K_{cat} values clearly show that the catalytic activity of Trx3C57S and Trx3C69S towards insulin decreased by 26% to 28% compared to the wild type (Table 2). Thus we concluded that both Cys57 and Cys69 also contribute to the activity of Trx3.

3.4. Superposition of yeast Trx3 against S-nitrosylated human Trx1

Sequence alignment of yeast Trx3 against human Trx1 indicated a proposed consensus motif of S-nitrosylation, (Arg/Lys/His/Glu/Asp)-Cys-(Asp/Glu) [39] around both Cys57 and Cys69 (Fig. 2A). A hydrophobic pocket close to the S-nitrosylated cysteines in human Trx1 has been proposed to be indispensable for the accessibility of the hydrophobic SNO group [10,40]. A similar hydrophobic pocket composed of residues Phe13, Ile25, Phe27 and Ile65 was also found around Cys69 in yeast Trx3. To have a better viewpoint, we superimposed this region of yeast Trx3 with the corresponding part of S-nitrosylated human Trx1, in which the S-nitrosylated cysteines are termed Snc62′ and Snc69′ (Fig. 2B). The residue Cys69 of Trx3 could be finely superimposed to Snc69′ of human Trx1, whereas Ser62 and Cys57 were superimposed to Snc62 and Val57′, respectively. Thus we supposed that Cys69 of Trx3 might involve in a similar S-nitrosylation reaction like its human homolog.

3.5. Residue Cys69 but not Cys57 could be S-nitrosylated in vitro

To further validate the above superposition results, we performed an in vitro S-nitrosylation of Trx3 with GSNO. The spectrum of GSNO-treated Trx3 presented a saturated absorbance peak at 335 nm (see the Supplementary materials), indicating the full S-nitrosylation of the oxidized Trx3 (Trx3-ox). The molar ratio of SNO/Trx3 is 0.92 as determined by Saville–Griess assay, suggesting only one thiol group of Trx3 was S-nitrosylated (Table 3). To further locate this S-nitrosylated site, the mutants of Trx3 (C57S and C69S) were also purified and analyzed. The mutant Trx3C57S has an S-nitrosylation ratio of 0.83, close to that of the wild type Trx3, whereas Trx3C69S could be S-nitrosylated at a ratio of 0.13 (Table 3). These results indicated that only Cys69 but not Cys57 could be S-nitrosylated in vitro, which is in agreement with the prediction from structural superposition (Fig. 2B).

Table 3
Representative SNO measurements

	Trx3	Trx3C57S	Trx3C69S
Sample (µM)	87.34	87.55	97.96
SNO/Trx3 molar ratio (Griess/Saville)	0.92	0.83	0.13

To verify whether S-nitrosylation of Cys69 affects the activity of Trx3, we also analyzed the kinetic data of GSNO-treated Trx3 based on their reduction activity towards insulin. As shown in Table 3, S-nitrosylation of Cys69 will decrease the activity of Trx3 by 36%, which is in accordance with the recent results of its S-nitrosylated counterpart in human Trx1 [9]. Interestingly, the effect of S-nitrosylation is comparable to that of Cys69Ser mutation. Recent reports indicated that non-active site residue Cys73 in human Trx1 could also function as an NO donor to promote S-nitrosylation of proteins [9,41,42]. Moreover, studies on human mitochondrial Trx2 suggested that its active site cysteine residues are responsible for protein denitrosylation [43]. These findings further suggested the potential relevance of the cysteine residues (both the additional ones and those at the active site) to the SNO modification.

Taken together, comparative structure analyses of yeast Trx3 revealed a significant redox-correlated conformational change of the additional cysteine residues Cys57 and Cys69 besides the active site. Moreover, Cys69 could be finely superimposed to a counterpart S-nitrosylated cysteine residue of human Trx1. In vitro S-nitrosylation in combination with site-directed mutageneses and activity assays further indicated the S-nitrosylated Cys69 could mimic the Cys69Ser mutation. These findings provided us some hints about the putative function of the additional cysteine residues of Trx3. However, details about the yeast mitochondrial NO production and its possible relation to Trx3 remain unclear, and more investigations in vivo are needed.

Acknowledgments

Appendix A. Supplementary data

Supplementary data associated with this article can be found, in the online version, at doi:10.1016/j.bbapap.2008.12.016.

References

[1] T.C. Laurent, E.C. Moore, P. Reichard, Enzymatic synthesis of deoxyribonucleotides. Iv. Isolation and characterization of thioredoxin, the hydrogen donor from *Escherichia coli* B, J. Biol. Chem. 239 (1964) 3436–3444.

[2] H. Schenk, M. Klein, W. Erdbrugger, W. Droge, K. Schulze-Osthoff, Distinct effects of thioredoxin and antioxidants on the activation of transcription factors NF-kappa B and AP-1, Proc. Natl. Acad. Sci. U. S. A. 91 (1994) 1672–1676.

[3] M. Russel, P. Model, The role of thioredoxin in filamentous phage assembly. Construction, isolation, and characterization of mutant thioredoxins, J. Biol. Chem. 261 (1986) 14997–15005.

[4] J. Chartron, C. Shiau, C.D. Stout, K.S. Carroll, 3'-Phosphoadenosine-5'-phosphosulfate reductase in complex with thioredoxin: a structural snapshot in the catalytic cycle, Biochemistry 46 (2007) 3942–3951.

[5] T. Yoshida, S. Oka, H. Masutani, H. Nakamura, J. Yodoi, The role of thioredoxin in the aging process: involvement of oxidative stress, Antioxid. Redox. Signal. 5 (2003) 563–570.

[6] K. Pekkari, M.T. Goodarzi, A. Scheynius, A. Holmgren, J. Avila-Carino, Truncated thioredoxin (Trx80) induces differentiation of human CD14+ monocytes into a novel cell type (TAMs) via activation of the MAP kinases p38, ERK, and JNK, Blood 105 (2005) 1598–1605.

[7] A. Holmgren, Thioredoxin, Annu. Rev. Biochem. 54 (1985) 237–271.

[8] J. Haendeler, J. Hoffmann, V. Tischler, B.C. Berk, A.M. Zeiher, S. Dimmeler, Redox regulatory and anti-apoptotic functions of thioredoxin depend on S-nitrosylation at cysteine 69, Nat. Cell. Biol. 4 (2002) 743–749.

[9] S.I. Hashemy, A. Holmgren, Regulation of the catalytic activity and structure of human thioredoxin 1 via oxidation and S-nitrosylation of cysteine residues, J. Biol. Chem. 283 (2008) 21890–21898.

[10] A. Weichsel, J.L. Brailey, W.R. Montfort, Buried S-nitrosocysteine revealed in crystal structures of human thioredoxin, Biochemistry 46 (2007) 1219–1227.

[11] B. Almeida, S. Buttner, S. Ohlmeier, A. Silva, A. Mesquita, B. Sampaio-Marques, N.S. Osorio, A. Kollau, B. Mayer, C. Leao, J. Laranjinha, F. Rodrigues, F. Madeo, P. Ludovico, NO-mediated apoptosis in yeast, J. Cell. Sci. 120 (2007) 3279–3288.

[12] P.R. Castello, P.S. David, T. McClure, Z. Crook, R.O. Poyton, Mitochondrial cytochrome oxidase produces nitric oxide under hypoxic conditions: implications for oxygen sensing and hypoxic signaling in eukaryotes, Cell. Metab. 3 (2006) 277–287.

[13] N. Cassanova, K.M. O'Brien, B.T. Stahl, T. McClure, R.O. Poyton, Yeast flavohemoglobin, a nitric oxide oxidoreductase, is located in both the cytosol and the mitochondrial matrix: effects of respiration, anoxia, and the mitochondrial genome on its intracellular level and distribution, J. Biol. Chem. 280 (2005) 7645–7653.

[14] L. Liu, M. Zeng, A. Hausladen, J. Heitman, J.S. Stamler, Protection from nitrosative stress by yeast flavohemoglobin, Proc. Natl. Acad. Sci. U. S. A. 97 (2000) 4672–4676.

[15] N.S. Osorio, A. Carvalho, A.J. Almeida, S. Padilla-Lopez, C. Leao, J. Laranjinha, P. Ludovico, D.A. Pearce, F. Rodrigues, Nitric oxide signaling is disrupted in the yeast model for Batten disease, Mol. Biol. Cell. 18 (2007) 2755–2767.

[16] C.M. Wong, Y. Zhou, R.W. Ng, H.F. Kung Hf, D.Y. Jin, Cooperation of yeast peroxiredoxins Tsa1p and Tsa2p in the cellular defense against oxidative and nitrosative stress, J. Biol. Chem. 277 (2002) 5385–5394.

[17] L. Liu, A. Hausladen, M. Zeng, L. Que, J. Heitman, J.S. Stamler, A metabolic enzyme for S-nitrosothiol conserved from bacteria to humans, Nature 410 (2001) 490–494.

[18] J.R. Pedrajas, E. Kosmidou, A. Miranda-Vizuete, J.A. Gustafsson, A.P. Wright, G. Spyrou, Identification and functional characterization of a novel mitochondrial thioredoxin system in *Saccharomyces cerevisiae*, J. Biol. Chem. 274 (1999) 6366–6373.

[19] R. Bao, Y.X. Chen, Y. Zhang, C.Z. Zhou, Expression, purification, crystallization and preliminary X-ray diffraction analysis of mitochondrial thioredoxin Trx3 from *Saccharomyces cerevisiae*, Acta Crystallograph. Sect. F. Struct. Biol. Cryst. Commun. 62 (2006) 1161–1163.

[20] T.A. Kunkel, Rapid and efficient site-specific mutagenesis without phenotypic selection, Proc. Natl. Acad. Sci. U. S. A. 82 (1985) 488–492.

[21] A.G. Leslie, Integration of macromolecular diffraction data, Acta Crystallogr. D. Biol. Crystallogr. 55 (1999) 1696–1702.

[22] C.C. Project, The CCP4 suite: programs for protein crystallography, Acta. Crystallogr. D. Biol. Crystallogr. 50 (1994) 760–763.

[23] A.T. Brunger, P.D. Adams, G.M. Clore, W.L. DeLano, P. Gros, R.W. Grosse-Kunstleve, J.S. Jiang, J. Kuszewski, M. Nilges, N.S. Pannu, R.J. Read, L.M. Rice, T. Simonson, G.L. Warren, Crystallography and NMR system: a new software suite for macromolecular structure determination, Acta Crystallogr. D. Biol. Crystallogr. 54 (1998) 905–921.

[24] T.A. Jones, J.Y. Zou, S.W. Cowan, M. Kjeldgaard, Improved methods for building protein models in electron density maps and the location of errors in these models, Acta Crystallogr. A. 47 (Pt 2) (1991) 110–119.

[25] C. Castro, F.A. Ruiz, I. Perez-Mato, M.M. Sanchez del Pino, L. LeGros, A.M. Geller, M. Kotb, F.J. Corrales, J.M. Mato, Creation of a functional S-nitrosylation site in vitro by single point mutation, FEBS Lett. 459 (1999) 319–322.

[26] I. Guevara, J. Iwanejko, A. Dembinska-Kiec, J. Pankiewicz, A. Wanat, P. Anna, I. Golabek, S. Bartus, M. Malczewska-Malec, A. Szczudlik, Determination of nitrite/nitrate in human biological material by the simple Griess reaction, Clin. Chim. Acta 274 (1998) 177–188.

[27] L.C. Green, D.A. Wagner, J. Glogowski, P.L. Skipper, J.S. Wishnok, S.R. Tannenbaum, Analysis of nitrate, nitrite, and [15N]nitrate in biological fluids, Anal. Biochem. 126 (1982) 131–138.

[28] A. Holmgren, Reduction of disulfides by thioredoxin. Exceptional reactivity of insulin and suggested functions of thioredoxin in mechanism of hormone action, J. Biol. Chem. 254 (1979) 9113–9119.

[29] R. Bao, Y. Chen, Y.J. Tang, J. Janin, C.Z. Zhou, Crystal structure of the yeast cytoplasmic thioredoxin Trx2, Proteins 66 (2007) 246–249.

[30] A. Weichsel, J.R. Gasdaska, G. Powis, W.R. Montfort, Crystal structures of reduced, oxidized, and mutated human thioredoxins: evidence for a regulatory homodimer, Structure 4 (1996) 735–751.

[31] M.C. Wahl, A. Irmler, B. Hecker, R.H. Schirmer, K. Becker, Comparative structural analysis of oxidized and reduced thioredoxin from *Drosophila melanogaster*, J. Mol. Biol. 345 (2005) 1119–1130.

[32] G. Capitani, Z. Markovic-Housley, G. DelVal, M. Morris, J.N. Jansonius, P. Schurmann, Crystal structures of two functionally different thioredoxins in spinach chloroplasts, J. Mol. Biol. 302 (2000) 135–154.

[33] A. Smeets, C. Evrard, M. Landtmeters, C. Marchand, B. Knoops, J.P. Declercq, Crystal structures of oxidized and reduced forms of human mitochondrial thioredoxin 2, Protein Sci. 14 (2005) 2610–2621.

[34] R. Friemann, H. Schmidt, S. Ramaswamy, M. Forstner, R.L. Krauth-Siegel, H. Eklund, Structure of thioredoxin from *Trypanosoma brucei brucei*, FEBS Lett. 554 (2003) 301–305.

[35] M. Saarinen, F.K. Gleason, H. Eklund, Crystal structure of thioredoxin-2 from *Anabaena*, Structure 3 (1995) 1097–1108.

[36] T. Kortemme, T.E. Creighton, Ionisation of cysteine residues at the termini of model alpha-helical peptides. Relevance to unusual thiol pKa values in proteins of the thioredoxin family, J. Mol. Biol. 253 (1995) 799–812.

[37] W.H. Watson, J. Pohl, W.R. Montfort, O. Stuchlik, M.S. Reed, G. Powis, D.P. Jones, Redox potential of human thioredoxin 1 and identification of a second dithiol/disulfide motif, J. Biol. Chem. 278 (2003) 33408–33415.

[38] J.F. Andersen, D.A. Sanders, J.R. Gasdaska, A. Weichsel, G. Powis, W.R. Montfort, Human thioredoxin homodimers: regulation by pH, role of aspartate 60, and crystal structure of the aspartate 60 -> asparagine mutant, Biochemistry 36 (1997) 13979–13988.

[39] J.S. Stamler, E.J. Toone, S.A. Lipton, N.J. Sucher, (S)NO signals: translocation, regulation, and a consensus motif, Neuron 18 (1997) 691–696.

[40] R. Sengupta, S.W. Ryter, B.S. Zuckerbraun, E. Tzeng, T.R. Billiar, D.A. Stoyanovsky, Thioredoxin catalyzes the denitrosation of low-molecular mass and protein S-nitrosothiols, Biochemistry 46 (2007) 8472–8483.

[41] D.A. Mitchell, S.U. Morton, N.B. Fernhoff, M.A. Marletta, Thioredoxin is required for S-nitrosation of procaspase-3 and the inhibition of apoptosis in Jurkat cells, Proc. Natl. Acad. Sci. U. S. A. 104 (2007) 11609–11614.

[42] D.A. Mitchell, M.A. Marletta, Thioredoxin catalyzes the S-nitrosation of the caspase-3 active site cysteine, Nat. Chem. Biol. 1 (2005) 154–158.

[43] M. Benhar, M.T. Forrester, D.T. Hess, J.S. Stamler, Regulated protein denitrosylation by cytosolic and mitochondrial thioredoxins, Science 320 (2008) 1050–1054.

[44] W.L. DeLano, The PyMOL User's Manual Palo Alto, CA, USA, 2002.

[45] P. Gouet, E. Courcelle, D.I. Stuart, F. Metoz, ESPript: analysis of multiple sequence alignments in PostScript, Bioinformatics 15 (1999) 305–308.

[46] J.D. Thompson, D.G. Higgins, T.J. Gibson, CLUSTAL W: improving the sensitivity of progressive multiple sequence alignment through sequence weighting, position-specific gap penalties and weight matrix choice, Nucleic Acids Res. 22 (1994) 4673–4680.